

Supplementary Information

Melt-Preparation of Organic-Inorganic Mn-Based Halide Transparent Ceramic Scintillators for High-Resolution X-ray Imaging

Zhi-Zhong Zhang,^{a**b**} Zi-Lin He,^b Qing-Peng Peng,^b Jing-Hua Chen,^b Bang Lan^a and Dai-Bin Kuang^{*b}

Z.Z. Zhang, B. Lan

[a] Northeast Guangdong Key Laboratory of New Functional Materials, School of Chemistry and Environment, Jiaying University, Meizhou, 514015, P.R. China.

Z.Z. Zhang, Z.L. He, Q.P. Peng, J.H. Chen, D.B. Kuang

[b] Key Laboratory of Bioinorganic and Synthetic Chemistry of Ministry of Education, LIFM, GBRCE for Functional Molecular Engineering, School of Chemistry, IGCME, Sun Yat-Sen University, Guangzhou 510275, China.

E-mail: kuangdb@mail.sysu.edu.cn

Experimental Section

Materials

Manganese bromide (MnBr_2 , Aladdin, 99.9%), Tetrabutylphosphonium bromide (TBPBr, Macklin, 98 %), hydrobromic acid (HBr, Aladdin, 48 weight% in water). The commercial scintillators of $\text{Lu}_3\text{Al}_5\text{O}_{12}$: Ce^{3+} (LuAG) and $\text{Bi}_4\text{Ge}_3\text{O}_{12}$ (BGO) crystals were purchased from EPIC Crystal Inc.

Preparation and growth of $\text{TBP}_2\text{MnBr}_4$ single crystals

The $\text{TBP}_2\text{MnBr}_4$ single crystals were grown by the solution volatilization method. The raw materials of 2 mmol TBPBr and 1 mmol MnBr_2 were dissolved in 5 mL HBr solution. Then, the solution was kept at 60 °C 5 h, then free cooling to room temperature, and the $\text{TBP}_2\text{MnBr}_4$ single crystals were obtained after 24 h.

Characterization of crystal structure

The single-crystal X-ray diffraction data of $\text{TBP}_2\text{MnBr}_4$ was collected through an Agilent Technologies Gemini A Ultra system. The crystal structure of $\text{TBP}_2\text{MnBr}_4$ was solved by using the SHELXTL and Olex2 program package,¹ and the structure symmetry was verified by the PLATON program.² Crystal structure refinement results are listed in Tables S1-S6. The CCDC numbers of $\text{TBP}_2\text{MnBr}_4$ crystallographic data are 2354948.

Measurements and characterizations

The powder XRD patterns of $\text{TBP}_2\text{MnBr}_4$ crystal and TC were performed on a Miniflex600 diffractometer (Rigaku). Steady-state PL and time-resolved PL spectra were measured by an FLS980 spectrometer (Edinburgh Instruments Ltd.). The light transmittance spectrum of the $\text{TBP}_2\text{MnBr}_4$ -TC was collected by using the UV-3600 spectrophotometer (Shimadzu). The PLQY value of $\text{TBP}_2\text{MnBr}_4$ crystal and TC were obtained on a Hamamatsu C9920 PLQY measurement system equipped with an integrated sphere. TGA was carried out on a TG209F1 Libra TGA system under an N_2 atmosphere. Differential scanning calorimetry (DSC) analysis was carried out on the

Netzsch DSC 214 instrument under an N₂ atmosphere at a heating/cooling rate of 10 K/min.

Viscosity Measurements

Temperature-dependent viscosity tests of the TBP₂MnBr₄ were carried out on a HAAKE MARS60 rotary rheometer. The sample was preheated to 150 °C to form a molten liquid and then cooled down at a rate of 5 °C min⁻¹, the viscosity values and shear stress were recorded.

Synthesis of TBP₂MnBr₄-TC

The TBP₂MnBr₄ crystals were placed in a beaker and heated at 130 °C for 30 minutes on a heating plate to form a homogeneous melt. Then, the melt was poured into the preheated crystallizing dish and naturally cooled to room temperature, forming a homogeneous and transparent TBP₂MnBr₄-TC.

Scintillation performance

The X-ray attenuation efficiency of TBP₂MnBr₄ was calculated by the formula:

$AE = (1 - e^{-t\rho d}) \times 100\%$. The attenuation coefficient (t) obtained from the XCOM database of the National Institute of Standards and Technology (NIST), ρ is the density, and d is the thickness of the TBP₂MnBr₄ scintillators. The radioluminescence spectra, relative light yields, and limit of radiation detection measurements were conducted according to the reported methods.^{3,4} The light yield (LY) is calculated from Equation:

$$\begin{aligned} LY(\text{Sample})/LY(\text{BGO}) \\ = (\alpha(\text{BGO}) \int I(\text{Sample})(\lambda) d\lambda) / (\alpha(\text{Sample}) \int I(\text{BGO})(\lambda) d\lambda). \end{aligned}$$

Where α is the absorption coefficient and $I(\lambda)$ is the radioluminescence spectra by Ocean Optics QE65pro portable spectrometer.

Table S1. Crystal data and structure refinement for TBP₂MnBr₄.

Empirical formula	C ₃₂ H ₇₂ P ₂ MnBr ₄
Formula weight	893.428
Temperature/K	138.61
Crystal system	monoclinic
Space group	<i>P</i> 2 ₁ /c
<i>a</i> /Å	17.1677(7)
<i>b</i> /Å	16.3806(8)
<i>c</i> /Å	17.4132(8)
$\alpha/^\circ$	90
$\beta/^\circ$	118.325(2)
$\gamma/^\circ$	90
Volume/Å ³	4310.6(4)
<i>Z</i>	4
ρ_{calc} g/cm ³	1.377
μ/mm^{-1}	4.106
F(000)	1835.4
Radiation	Mo K α ($\lambda = 0.71073$)
2 Θ range for data collection/°	4.68 to 55.02
Index ranges	-22 ≤ <i>h</i> ≤ 22, -19 ≤ <i>k</i> ≤ 21, -22 ≤ <i>l</i> ≤ 22
Reflections collected	50696
Independent reflections	9907 [$R_{\text{int}} = 0.0799$, $R_{\text{sigma}} = 0.0629$]
Data/restraints/parameters	9907/0/371
Goodness-of-fit on F ²	1.014
Final <i>R</i> indexes [I>=2σ (I)] ^a	$R_1 = 0.0421$, $wR_2 = 0.0921$
Final <i>R</i> indexes [all data] ^a	$R_1 = 0.0687$, $wR_2 = 0.1051$
Largest diff. peak/hole / e Å ⁻³	2.15/-1.37

^a $R_1 = \sum |F_o| - |F_c| / \sum |F_o|$ and $wR_2 = [\sum w(F_o^2 - F_c^2)^2 / \sum w F_o^4]^{1/2}$ for $F_o^2 > 2\sigma(F_o^2)$

Table S2. Fractional atomic coordinates ($\times 10^4$) and equivalent isotropic displacement parameters ($\text{\AA}^2 \times 10^3$) for TBP₂MnBr₄.

Atom	x	y	z	U(eq)
Br01	1297.8(3)	11623.7(2)	7947.4(3)	37.03(11)
Br02	2584.2(2)	9456.5(3)	8387.4(2)	38.60(11)
Br03	1800.7(3)	10543.1(3)	6070.8(2)	40.56(11)
Br04	3811.9(4)	11607.6(5)	8122.0(18)	43.5(5)
Br1	3787.1(16)	11533(2)	8527(6)	48.6(14)
Mn05	2386.0(3)	10827.9(3)	7660.6(4)	31.64(14)
P006	4440.5(6)	3831.7(6)	6068.9(6)	28.9(2)
P007	332.7(6)	10667.6(6)	3374.6(6)	29.1(2)
C008	1383(2)	11188(2)	3791(2)	29.2(8)
C009	4935(2)	3754(2)	7240(2)	29.8(8)
C00A	2817(2)	3379(2)	5999(3)	34.6(8)
C00B	4275(3)	4893(2)	5759(2)	33.5(8)
C00C	421(2)	9716(2)	3926(3)	33.6(8)
C00D	5159(3)	3401(2)	5685(3)	34.5(8)
C00E	-397(2)	11289(2)	3612(3)	34.6(8)
C00F	1131(2)	9127(2)	3987(2)	33.1(8)
C00G	2034(2)	10891(2)	3480(2)	35.5(9)
C00H	3927(3)	5413(2)	6263(2)	32.9(8)
C00I	3737(2)	6288(2)	5942(2)	33.5(8)
C00J	5870(2)	4122(2)	7719(2)	33.9(8)
C00K	5390(3)	2503(2)	5936(3)	40.3(10)
C00L	3408(3)	3276(3)	5574(3)	40.8(10)
C00M	-1260(3)	10202(3)	268(2)	40.1(9)
C00N	1101(3)	8336(2)	4427(3)	39.6(9)
C00O	1991(3)	2852(3)	5564(3)	41.5(10)
C00P	-1111(3)	12647(2)	3565(3)	42.3(10)
C00Q	-592(3)	12148(3)	3234(3)	44.3(10)
C00R	2888(2)	11374(2)	3896(3)	38.5(9)
C00S	-96(3)	10399(3)	2238(2)	40.9(9)
C00T	6172(3)	4268(3)	8686(2)	43.0(10)
C00U	1828(3)	7748(3)	4533(3)	44.5(10)
C00V	3523(3)	6810(3)	6532(3)	51.5(12)
C00W	6062(3)	2184(2)	5681(3)	45.0(10)
C00X	-444(3)	10744(3)	704(2)	43.8(10)
C00Y	6297(3)	1294(3)	5935(3)	50.3(11)
C00Z	-285(3)	11081(3)	1605(3)	42.9(10)
C010	1410(3)	2938(3)	5994(3)	52.5(12)
C011	3560(3)	11078(3)	3620(3)	48.4(11)
C012	5744(3)	5013(3)	8851(3)	58.6(13)
C013	-1255(4)	13524(3)	3241(3)	56.5(13)

Table S3. Atomic occupancy for $\text{TB}_{\text{P}2}\text{MnBr}_4$.

Atom	Occupancy	Atom	Occupancy
Br04	0.772(8)	Br1	0.228(8)

Table S4. Bond lengths for TBP₂MnBr₄.

Atom	Atom	Length/Å
Br01	Mn05	2.5149(7)
Br02	Mn05	2.5210(7)
Br03	Mn05	2.5002(7)
Br04	Mn05	2.5304(11)
Mn05	Br1	2.439(2)

Table S5. Bond angles for TBP₂MnBr₄.

Atom	Atom	Atom	Angle/°
Br02	Mn05	Br01	107.35(2)
Br03	Mn05	Br01	111.74(2)
Br03	Mn05	Br02	106.10(2)
Br04	Mn05	Br01	111.91(4)
Br04	Mn05	Br02	114.24(4)
Br04	Mn05	Br03	105.41(7)
Br1	Mn05	Br01	103.86(14)
Br1	Mn05	Br02	104.64(17)
Br1	Mn05	Br03	122.2(3)

Table S6. Hydrogen bonds for TBP₂MnBr₄.

D	H	A	d(D-H)/Å	d(H-A)/Å	d(D-A)/Å	<(D-H-A)/°
C008	H1	Br01 ¹	0.99	2.901(3)	3.850(4)	160.90(7)
C008	H	Br03	0.99	2.931(3)	3.833(3)	151.92(7)
C00B	H00e	Br02 ²	0.99	2.945(4)	3.904(4)	163.24(7)
C00B	H00f	Br1 ³	0.99	3.097(5)	3.988(5)	150.38(17)
C00C	H2	Br01 ⁴	0.99	3.040(4)	3.877(4)	143.06(7)
C00C	H2	Br03 ⁴	0.99	3.110(4)	3.841(4)	131.81(7)
C00C	Ha	Br03	0.99	2.784(4)	3.605(4)	140.77(7)
C00D	H00g	Br02 ³	0.99	2.846(4)	3.830(4)	172.59(7)
C00D	H00h	Br04 ²	0.99	2.954(5)	3.934(5)	170.88(8)
C00D	H00h	Br1 ²	0.99	2.401(9)	3.360(9)	162.96(19)
C00E	Hb	Br02 ⁴	0.99	3.118(4)	3.912(4)	138.14(7)
C00I	H00k	Br04 ³	0.99	2.921(4)	3.759(4)	143.03(9)
C00I	H00k	Br1 ³	0.99	3.019(5)	3.919(5)	151.72(12)
C00L	H00q	Br1 ²	0.99	3.261(11)	3.929(11)	126.30(9)
C00O	H00s	Br03 ⁵	0.99	3.104(4)	3.932(4)	142.07(8)
C00R	Hj	Br1 ¹	0.99	3.164(8)	3.936(5)	135.91(10)
C00S	H11	Br01 ⁴	0.99	3.015(4)	3.835(4)	140.95(8)
C00S	H11	Br02 ⁴	0.99	3.121(4)	3.882(4)	134.75(8)
C00T	H00v	Br03 ³	0.99	3.123(4)	3.905(4)	136.98(7)

¹+X,5/2-Y,-1/2+Z; ²+X,3/2-Y,-1/2+Z; ³1-X,-1/2+Y,3/2-Z; ⁴-X,2-Y,1-Z; ⁵+X,-1+Y,+Z

Table S7. Comparison of scintillation performance of recently reported single-crystal/ceramic scintillators.

Materials	Type	Optical transparency	Light yield (photons/MeV)	Detection limit (nGy/s)	Imaging resolution (lp/mm)	Ref
TEA ₂ MnI ₄	crystal	90%	26288	10.1	25	3
(2-DMAP) ₂ MnBr ₄	crystal	93.6%	22000	76.35	20-25	5
(PEA) ₂ PbBr ₄	crystal	—	73226	40.4	11.1	6
Cs ₃ Cu ₂ Cl ₅	crystal	86%	95,000	2700	105	7
Y ₃ Al ₅ O ₁₂ :Ce ³⁺	ceramic	82%	24600	157.4	34.7	8
TPP ₂ MnBr ₄	ceramic	68%	78000	8.8	15.7	9
[C ₈ H ₂₀ N] ₂ Cu ₂ Br ₄	ceramic	—	91300	52.1	9.54	10
TBP ₂ MnBr ₄	ceramic	80 %	4840	516	16	This work

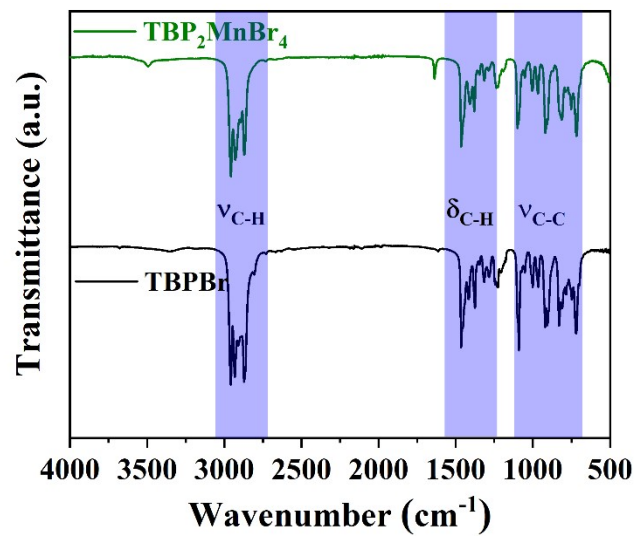


Figure S1. The infrared spectra of $\text{TBP}_2\text{MnBr}_4$ crystalline and TBPBr organic salts.

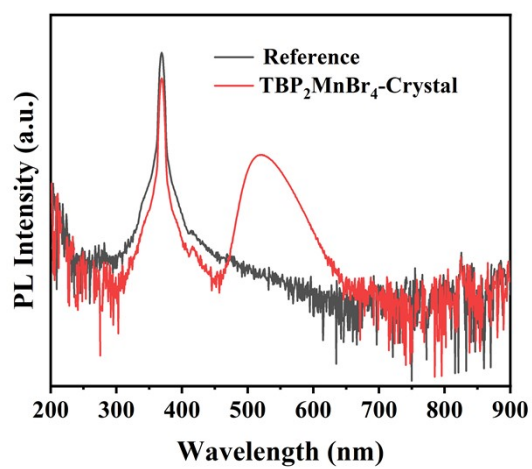


Figure S2. The PLQY curve of $\text{TBP}_2\text{MnBr}_4$ -crystal under 370 nm UV excitation.

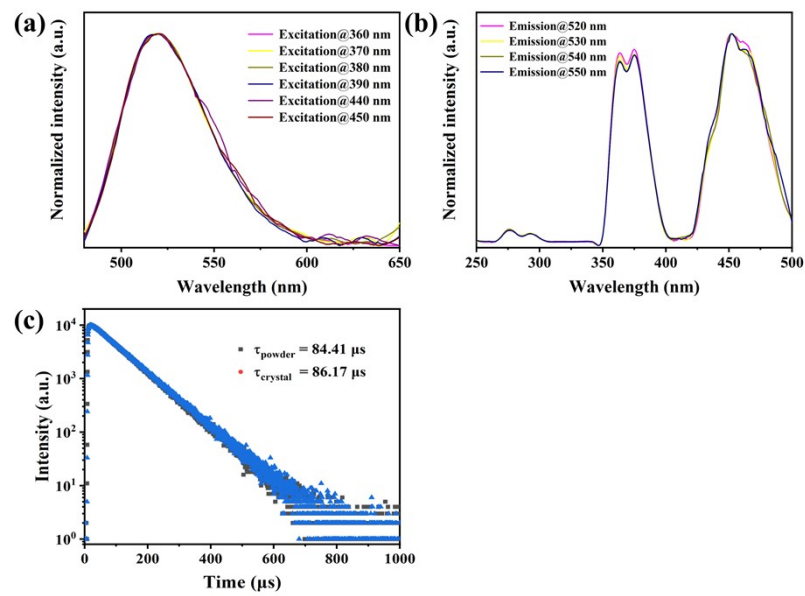


Figure S3. (a) Emission-wavelength-dependent PLE spectra of $\text{TBP}_2\text{MnBr}_4$ -crystal, (b) excitation-wavelength-dependent PL spectra of $\text{TBP}_2\text{MnBr}_4$ -crystal, (c) the TRPL spectra of polycrystalline powder and crystal of $\text{TBP}_2\text{MnBr}_4$ -crystal.

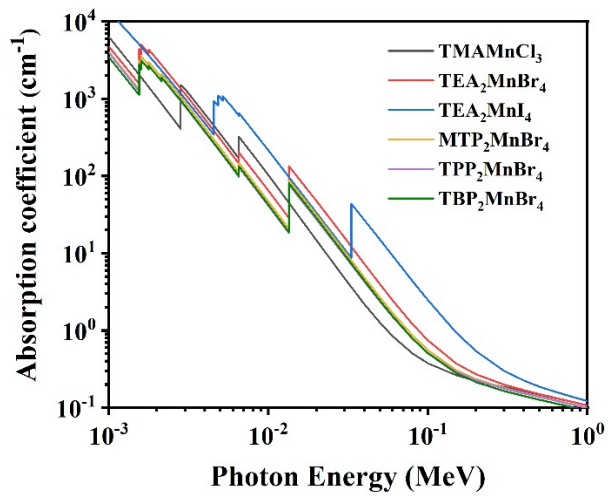


Figure S4. X-ray absorption coefficients plots for TBP₂MnBr₄ and other reported Mn(II)-based OIMHs as a function of photon energy.

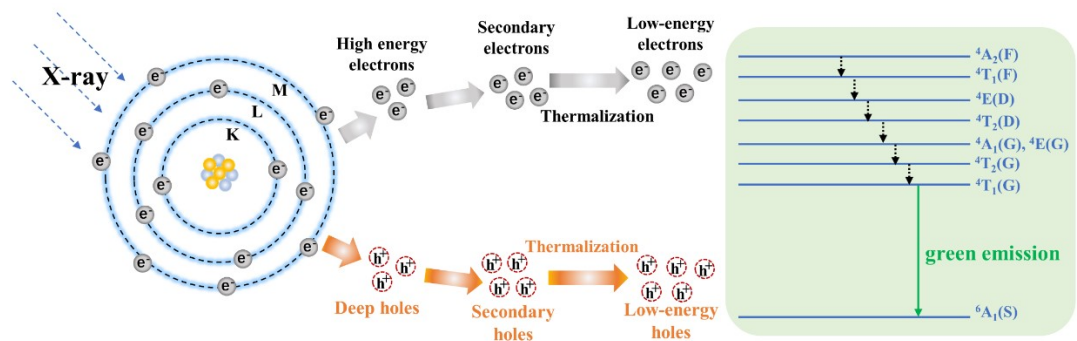


Figure S5. Schematic diagram of the scintillating mechanism.

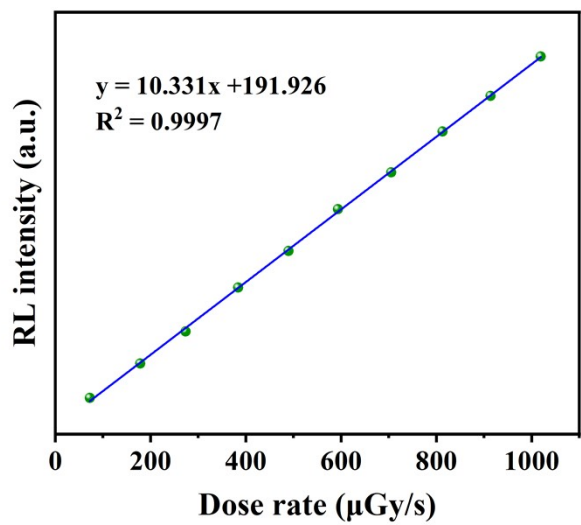


Figure S6. The linear relationship between the dose rate and RL intensity for $\text{TBP}_2\text{MnBr}_4$ -crystal.

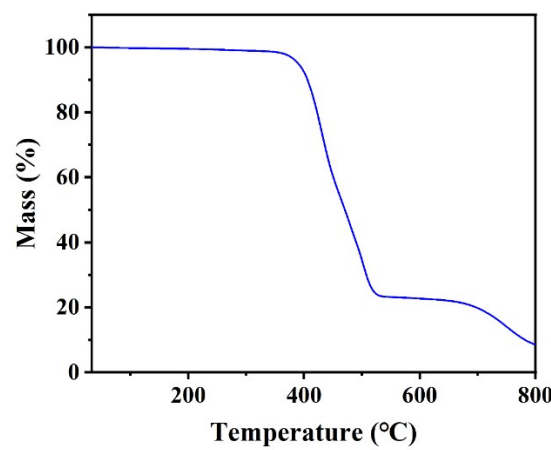


Figure S7. The TG curve of $\text{TBP}_2\text{MnBr}_4$ -crystal.

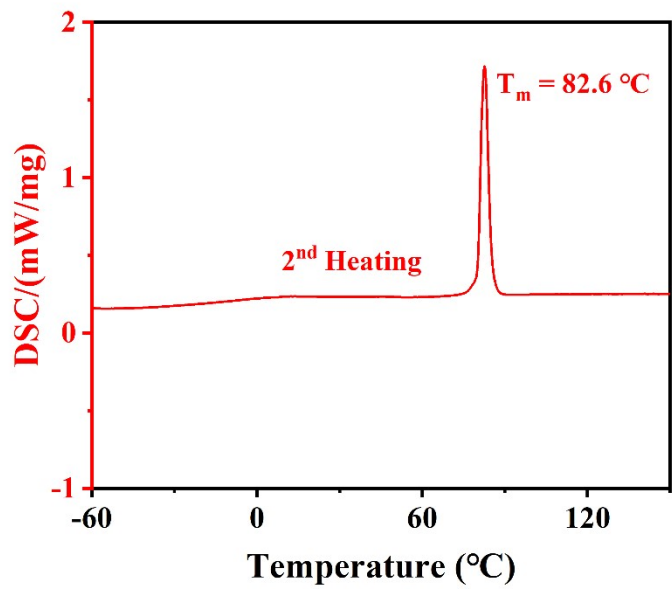


Figure S8. The DSC curve of $\text{TBP}_2\text{MnBr}_4$ -crystal for the secondary heating.

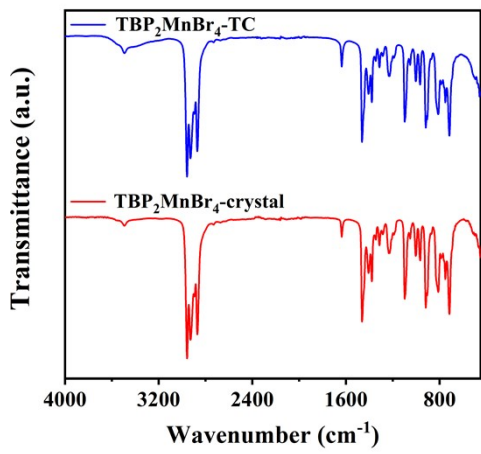


Figure S9. ATR-FTIR spectra of $\text{TBP}_2\text{MnBr}_4$ -crystal and $\text{TBP}_2\text{MnBr}_4$ -TC.

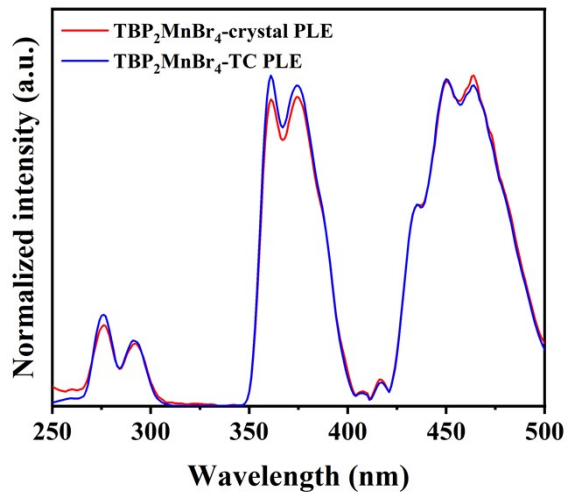


Figure S10. The PLE spectra of $\text{TBP}_2\text{MnBr}_4$ -crystal and $\text{TBP}_2\text{MnBr}_4$ -TC.

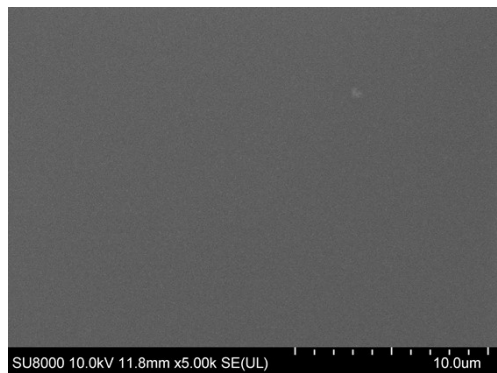


Figure S11. SEM image of $\text{TBP}_2\text{MnBr}_4$ -TC.

Reference

- 1 O. V. Dolomanov, L. J. Bourhis, R. J. Gildea, J. A. K. Howard, H. Puschmann, *J. Appl. Crystallogr.* 2009, **42**, 339.
- 2 A. L. Spek, *J. Appl. Crystallogr.* 2003, **36**, 7.
- 3 Z.-Z. Zhang, J.-H. Wei, J.-B. Luo, X.-D. Wang, Z.-L. He, D.-B. Kuang, *ACS Appl. Mater. Interfaces* 2022, **14**, 47913-47921.
- 4 J.-B. Luo, J.-H. Wei, Z.-Z. Zhang, Z.-L. He, D.-B. Kuang, *Angew. Chem. Int. Ed.* 2023, **62**, e202216504.
- 5 Z. L. He, J. H. Wei, Z. Z. Zhang, J. B. Luo and D. B. Kuang, *Adv. Optical Mater.*, 2023, **11**, 2300449.
- 6 B. X. Jia, D. P. Chu, N. Li, Y. X. Zhang, Z. Yang, Y. J. Hu, Z. Q. Zhao, J. S. Feng, X. D. Ren, H. Zhang, G. T. Zhao, H. M. Sun, N. Y. Yuan, J. N. Ding, Y. C. Liu and S. Z. Liu, *ACS Energy Lett.*, 2023, **8**, 590-599.
- 7 W. Xiang, D. Shen, X. Zhang, X. Li, Y. Liu and Y. Zhang, *ACS Appl. Mater. Interfaces*, 2024, **16**, 4918-4924.
- 8 T. Ji, T. Wang, H. Li, Q. Peng, H. Tang, S. Hu, A. Yakovlev, Y. Zhong and X. Xu, *Adv. Optical Mater.*, 2022, **10**, 2102056.
- 9 K. Han, K. Sakhatskyi, J. Jin, Q. Zhang, M. V. Kovalenko and Z. Xia, *Adv. Mater.*, 2022, **34**, 2110420.
- 10 B. Su, J. Jin, K. Han and Z. Xia, *Adv. Funct. Mater.*, 2022, **33**, 2210735.